First-Principles Free-Energy Analysis of Helix Stability: The Origin of the Low Entropy in π Helices

Lars Ismer,*[,†,‡] Joel Ireta,[†,§] and Jörg Neugebauer[‡]

Fritz-Haber-Institut der Max-Planck-Gesellschaft, Faradayweg 4-6, 14195 Berlin, Germany, Max-Planck-Institut für Eisenforschung GmbH, Max-Planck-Str. 1, 40237 Düsseldorf, Germany, and Departemento de Química, División de Ciencias Básicas e Ingeniería, Universidad Autónoma Metropolitana-Iztapalapa, San Rafael Atlixco 186, A.P. 55-534, 09340 México, D.F. México

Received: September 26, 2007; In Final Form: December 19, 2007

The temperature dependence of the stability of infinite poly-L-alanine α, π, and 3_{10} helices with respect to the fully extended structure (FES) is calculated using density functional theory and the harmonic approximation. We find that the vibrational entropy strongly reduces the stability of the helical conformations with respect to the FES. By mapping the ab initio data on an approximate mechanical model, we show that this effect is exclusively due to the formation of hydrogen bonds, whereas changes in the backbone stiffness are practically negligible. We furthermore observe that the temperature dependence is largest for the π helix and smallest for the 3_{10} helix and demonstrate that these trends are a generic behavior related to the geometric peculiarities of the respective helical conformations and independent of the specific amino acid sequence.

Approximately 90% of the residues in known proteins are found in locally regular conformations such as helices, sheets, and turns.[1] The helix is the most abundant of these conformational motifs. Three different types have been found in proteins: the 3_{10}, α, and π helices, which differ in the number of residues per turn and the hydrogen bonding (hb) pattern they form (Figure 1). In the 3_{10} helix, 3.12 residues are needed to form a helical turn, 3.66 in the α helix, and 4.5 in the π helix. The hbs are formed between residues i and $i + \nu$, where $\nu = 3$ for the 3_{10} helix, $\nu = 4$ for the α helix, and $\nu = 5$ for the π helix. In protein crystals, the α helix is the predominant type with an occurrence of ∼80 % followed by the 3_{10} helix with an occurrence of ∼20 %.[2] In contrast, extended π helices are found only in exceptional cases.[3] However, π-helix-like conformations together with 3_{10}-helical motifs are known to be common deformations at the end of α helices in protein crystals.[4] Furthermore, investigations on the conformations of L-alanine-rich peptides in solution indicate that π- and 3_{10}-helical segments may be present as defects in α helices.[5,6] Recent experimental studies suggest that the presence of transient defect structures (i.e., the content of π- and 3_{10}-helical segments) in solvated α helices is larger at low temperatures (e.g., at ∼0 °C) than at high temperatures (e.g., at ∼30 °C). On the basis of these experimental findings, it has been concluded that the melting temperature for π and 3_{10} helices is lower than the melting temperature for an α helix.[5] This implies that the relative thermodynamic stability (which is given by the difference in the free energy of formation) between the three helix-types is not a constant but shows a strong temperature dependence. Furthermore, the fact that in the biological relevant temperature window all three helix types coexist indicates that the free energies are close to degeneracy. An accurate determination/understanding of the relative stability between the helical conformations is therefore crucial. An important question in this respect is whether the temperature dependence is caused by extrinsic parameters, for example, by modifications in the solvent interactions at lower temperatures,[5,6] or whether it is an intrinsic property of the helical structures. Conventionally, the relative stabilities intrinsic to the three helical conformations in *finite* peptides is discussed in terms of the total number of hbs they form: for a given finite chain length the 3_{10} helix forms one more hydrogen bond than the α helix; thus, the former should be energetically preferred, whereas the π helix forms one less hydrogen bond and is thus energetically handicapped. Furthermore, it has been suggested that the entropic cost of helix initiation is higher in π helices than in α helices (and correspondingly lower in 3_{10} helices) because a larger number of residues has to be aligned correctly to form the first hydrogen

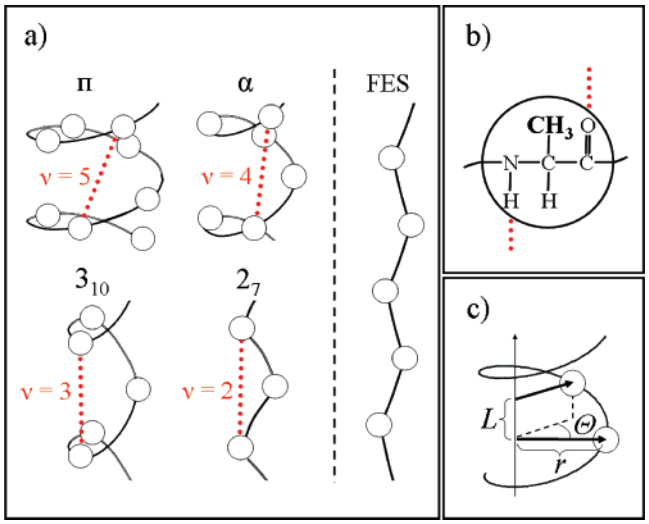

Figure 1. (a) Analyzed conformations of the peptide chain with their corresponding hydrogen-bonding patterns. The dotted lines denote N−H···O═C hydrogen bonds. (b) Sketch of the alanine residue. (c) Helical parameters as discussed in the text.

* Corresponding author. E-mail: ismer@mpie.de.
† Fritz-Haber-Institut der Max-Planck-Gesellschaft.
‡ Max-Planck-Institut für Eisenforschung GmbH.
§ Universidad Autónoma Metropolitana-Iztapalapa.

10.1021/jp077728n CCC: $40.75
Published on Web 03/08/2008

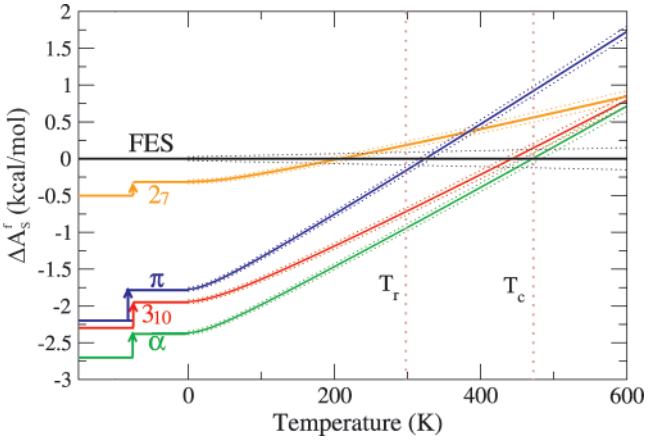

Figure 2. Stability per residue of different poly-L-alanine conformations with respect to FES as the temperature increases (eq 1). The dotted lines denote the numerical error bars. The arrows give the zero-point vibrational corrections. T_r and T_c stand for room temperature and critical temperature (see text), respectively.

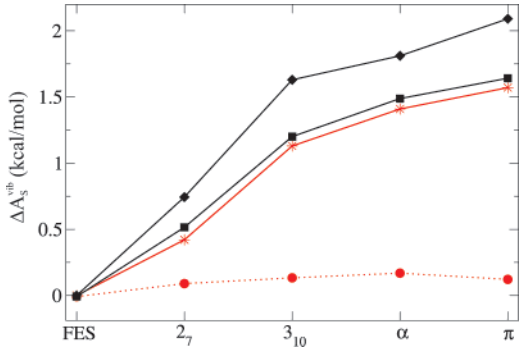

Figure 3. Vibrational free energy contributions to the stability of the conformations with respect to the FES, that is, $\Delta A_S^{vib}(T) = A_S^{vib}(T) - A_{FES}^{vib}(T)$, at room temperature. DFT results for the contributions from the full vibrational spectrum (continuous black line, diamonds). Contributions from the three lowest vibrational branches (continuous black line, squares). Contributions calculated using the ball and spring model with spring constants listed in Table 1 (continuous red line, stars). Contributions when the hydrogen-bonding spring constants are removed from the model (dotted red line, circles).

bond of the helix.[7] However, these differences do not apply for a residue in the middle of long peptides, that is, a situation in which dangling hbs are absent. We have therefore studied the temperature-dependent relative stability of *bulk*-like 3_{10}, α, and π helices using infinitely long L-alanine polypeptides. We have not included solvent or any environmental effects in our investigation because we aim to get a deeper insight into the *intrinsic* propensity of the bulk of a polypeptide to adopt different helical conformations.

For a reliable description of the rather delicate differences between the helix types, the proper choice of the theoretical method in use is of crucial importance. Traditionally, the treatment of temperature-dependent aspects of helix stability on the atomic scale is reserved to empirical force field simulations. It is, however, not clear whether or not the limited accuracy and predictive power of this approach allows one to reproduce the differences between the helix types accurately. Indeed, it has been shown that the relative stability of the helix types strongly depends on the chosen force field parametrization[8] and might be artificial for an individual force field. We have therefore completely based our analysis on density functional theory (DFT) in the generalized gradient approximation (GGA).

DFT-GGA studies of helices in vacuum have already been useful to unveil the role that hbs play in stabilizing the different helical conformations[9−12] at 0 K. In a previous publication, we determined the vibrational spectrum in the harmonic approximation for an infinitely long poly-L-alanine α helix[13] and compared it to experimental data as obtained from Raman and IR spectroscopy of crystalline α-helical poly-L-alanine in the group of Krimm.[14] An overall excellent agreement between the predicted and experimental frequencies has been obtained. Here, we employ DFT-GGA to compute the vibrations and the free energy of all experimentally observed helical conformations as well as of the fully extended structure (FES; see Figure 1), which lacks hbs and serves as a reference. Furthermore, we include the 2_7 conformation to complete the study in terms of possible hb patterns (Figure 1).

The infinite helices can be described as crystals with, in terms of cylindrical coordinates, a one-dimensional lattice periodicity: each lattice point n contains as a basis a L-alanine residue, which consists of $p = 10$ atoms at positions $u_{i\alpha}^{cyl}$, where i goes over the p atoms and α goes over the three cylindrical directions r, ϕ, and z. The lattice vector, which transforms one representative residue into its nth nearest neighbor is given by $\mathbf{R}_n^{cyl} = (0, n * \Theta, n * L)$. Here Θ is the helix twist and L is the helix pitch, that is, the increment per residue along the z axis (Figure 1c). The calculations have been performed using a plane wave pseudopotential approach as implemented in SFHIngX.[15] The peptide chain has been modeled in an orthorhombic supercell. All calculations have been performed using the Perdew, Burke, and Ernzerhoff (PBE) GGA functional,[16] and a plane wave energy cutoff of 70 Ry. Further details are given in refs 11, 13, 17.

All conformations studied here correspond to a minimum on the (Θ, L) potential-energy surface for an infinite L-alanine polypeptide with all internal degrees of freedom fully relaxed.[17] The cylindrical coordinates describing the equilibrium structures investigated here are Θ = 80°, 98.2°, 120.0°, 180.0°, and 180.0° and L = 1.17, 1.50, 1.97, 2.83, and 3.57 Å for the 3_{10}, α, and π helix, the 2_7 conformation, and the FES, respectively. The stability of a given conformation is referred to the Helmholtz free energy of the FES:

$$\Delta A_S^f(T) = A_S(T) - A_{FES}(T) \qquad (1)$$

Here $A_S(T)$ is the free energy per residue, where the subscript S specifies the conformation. $A_{FES}(T)$ is the free energy per residue of the FES. Following the Born−Oppenheimer and the harmonic approximation, $A_S(T)$ is given by

$$A_S(T) = U_S^{el} + A_S^{vib}(T) = U_S^{el} + U_S^{vib}(T) - T * S_S^{vib}(T) \qquad (2)$$

Here, U_S^{el} is the total energy per residue of the fully relaxed chain conformation, A_S^{vib} is the vibrational free energy per residue, and $S_S^{vib}(T)$ and $U_S^{vib}(T)$ denote the entropic and the enthalpic vibrational contributions per residue to the free energy, respectively. To determine the vibrational contributions to the free energy, we solve the secular equation for the symmetry-reduced dynamical matrix.[13] Great care has been taken to reduce the numerical error in the frequencies to less than 3 cm^{-1}; the numerical uncertainty in the vibrational free energy of the helices and the FES at 300 K is below 0.05 and 0.1 kcal/mol, respectively.

Employing this approach, $\Delta A_S^f(T)$ (eq 1) has been calculated (Figure 2). For the case of T = 0 K, all three helical

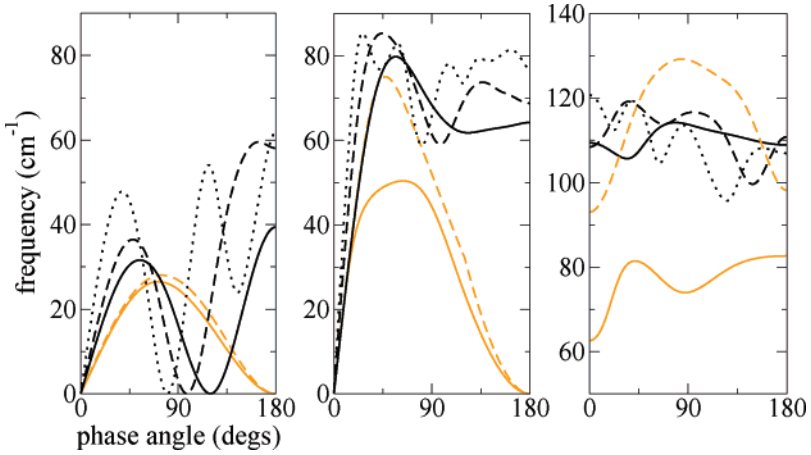

Figure 4. Lowest frequency branches of π (dotted dark), α (dashed dark), and 3_{10} helix (continuous dark), 2_7 conf. (dashed light), and FES (continuous light).

TABLE 1: Parameter Set for the Ball and Spring Model (eqs 3−5) and the Thin Rod Approximation (eqs 6−8) (The Spring Constants Are Expressed in cm^{-2} × 10^4)

	K_{r1}	K_δ	K_ϕ	$K_{r_{\nu-1}}$	K_{r_ν}	K_l	$K_{t,bb}$	$K_{t,hb}$
3_{10}, α, π	21.6	0.79	3.02	21.6	12.3	19.4	0.45	0.11
2_7	21.6	0.79	3.02	8.60	12.3			
FES	21.6	0.17	3.02					

conformations are energetically preferred over the FES, owing to the formation of hbs.[17] The same applies for the 2_7 conformation, although the energetic preference is much smaller for this conformation than for the helices. Among all conformations, the α helix is energetically most stable at $T = 0$ K. The π and the 3_{10} helix are energetically degenerate and slightly higher in energy (by ~0.5 kcal/mol per residue) than the α helix. As indicated by the arrows in Figure 2, the zero-point vibrational correction ΔU_S^{vib} (0 K) makes all helices slightly less stable with respect to the FES. However, the energetic ordering of the conformations remains. This result is consistent with the findings reported for the α helix in ref 18. For finite temperatures, a significant change in the relative stabilities is observed: the 2_7 conformation becomes unstable against the FES already for $T > 200$ K, and the π helix appears as the least favored of the three helical conformations at room temperature; it is almost degenerate to the FES. In contrast the α and 3_{10} helices are still energetically favored with respect to FES at room temperature by 0.9 and 0.6 kcal/mol per residue, respectively. At a critical temperature $T_c = 470$ K, the FES becomes the thermodynamically most favorable conformation. These results clearly reveal that vibrational entropy is sizable at temperatures relevant to the experimental observations affecting primarily the relative stability of the π helix as indicated by the slopes of the curves in Figure 2.

To understand the pronounced differences in the entropic character between helices and between helices and the FES, we have analyzed the vibrational entropy in detail. Our results show that at room temperature about 75% of the vibrational free energy differences arise from the three lowest vibrational branches (Figure 3; diamonds vs squares). These are the two acoustical and the first optical branches (Figure 4). The fact that only three branches determine the complex thermodynamic behavior allowed us to map the problem on a simple ball and spring model. Here, the peptides (amino acids) are considered as rigid units (balls) connected to each other by harmonic springs. The potential energy of the peptide chain is decomposed into contributions arising from the deformation of the backbone U^{bb} and hydrogen U^{hb} bonds. Together with the kinetic energy, T, the model Hamiltonian can be expressed as

$$H = T + U^{bb} + U^{hb} \tag{3}$$

$$U^{bb} = \frac{1}{2}\sum_n K_{r_1}|\Delta r_{n_1}|^2 + K_\phi|\Delta\phi_n|^2 + K_\delta|\Delta\delta_n|^2 \tag{4}$$

$$U^{hb} = \frac{1}{2}\sum_n K_{r_\nu}|\Delta r_{n_\nu}|^2 + Kr_{\nu-1}|\Delta r_{\nu-1}|^2 \tag{5}$$

The backbone contributions, U^{bb}, are modeled in terms of displacements in the bond distances Δr_{n_1}, the valence angles $\Delta\phi_n$, and the dihedral angles $\Delta\delta_n$ at residue n[19]). The backbone stiffness is contained in the spring constants K_r, K_ϕ, and K_δ. The hbs are modeled in terms of the distances between the peptides n and $n + \nu$ and between the peptides n and $n + \nu - 1$. The corresponding spring constants are K_{r_ν} and $K_{r_{\nu-1}}$. This approach is an extension of model Hamiltonians applied recently to study the propagation of solitons along helical polymers.[19,20] Although in ref 20 the hbs have been described by a single force constant, we found that an effective three-body treatment of the hydrogen bonding is essential to get an accurate fit to the low-frequency branches for the α and π helices, as calculated within the DFT-GGA approach. The nature of the three-body interaction is likely due to the large cooperativity and/or directionality of the hbs.[11]

Great care has been taken to ensure the maximum transferability and the physical significance of the optimized spring constants (details in ref 21). The parameter set thus obtained is listed in Table 1 and adequately reproduces the ab initio results (squares vs stars in Figure 3). By setting specific force constants to zero, the model allows us to quantify which bonds (hb or bb) determine the entropic character of the various conformations. By setting all hbs to zero (dots in Figure 3), the entropic differences between the conformations almost completely disappear. We can therefore conclude that the temperature effects are dominated by the hbs, whereas changes in the stiffness of the backbone due to the helix formation are practically negligible.

An interesting consequence of the ball and spring model is that the force constants are independent of the helix conformation (Table 1). It is therefore tempting to conclude that the entropic differences between the helices are purely geometric and thus generic. To discuss this aspect in more detail, a

mapping of the spring model onto a minimal mechanical model, the thin rod approximation, turned out to be useful. This model accurately reproduces the long-wavelength limit of the mechanical deformations of the helix and thus the dispersion in the low-energy phonon branches around the nodal ($\omega = 0$) points, which have been found to dominate the differences in the vibrational entropy. Using this approximation, the following dispersion relations have been derived (details in ref 21):

$$\omega^{l}(\varphi) = \nu \sqrt{\frac{K^{l,hb}}{M}}\,\varphi \tag{6}$$

$$\omega^{b}(\varphi) = \frac{R\nu}{2L} \sqrt{\frac{K^{l,hb}}{M}}\,(\varphi - \Theta)^2 \tag{7}$$

$$\omega^{t}(\varphi) = R \sqrt{\frac{K^{t,bb} + \nu^2 K^{t,hb}}{M}}\varphi \tag{8}$$

Here the superscripts l, b, and t stand for longitudinal (stretching), bending, and torsional waves, respectively. $K^{l,hb}$, $K^{t,hb}$, and $K^{t,bb}$ are effective force constants independent of the specific helix conformation (Table 1). M denotes the mass of the residue (72.1 Da for alanine). R denotes the radius of the helix, which we define as the distance of the center of mass of the residue to the helix axis, and is 1.96, 2.17, and 2.66 Å for the 3_{10}, α, and π helix, respectively. The subscript hb or bb indicates whether hb or bb related parameters enter in the calculation of the respective spring constants. A rather unexpected result arising from this analysis is that the propagation of longitudinal and bending waves occurs exclusively along the hbs; that is, eqs 6 and 7 do not depend on the constants associated to the backbone. The propagation of the torsional waves involves both backbone and hbs. We note, however, that also for the torsional waves the hbs dominate ($\nu^2 K^{t,hb} > K^{t,bb}$). A second interesting consequence is that because the π helix is unique with respect to all geometric aspects (the largest radius, the smallest pitch and the largest number of peptides ν bridged by the hbs) it directly exhibits the hardest response to elastic deformations (eqs 6−8). Because of this response, the π helix suffers a relative loss in vibrational entropy with respect to all other conformations.

In conclusion, our results shed light on the relative stability of secondary structure motifs at temperatures relevant to experimental observations. Our results on poly-L-alanine show that the vibrational entropy significantly reduces the stability of helices with respect to FES. This effect is strongest for π helices. Employing a minimum mechanical model for the helices, which correctly reproduces the low-energy long-wavelength modes dominating the thermodynamic properties, it has been demonstrated that the strong temperature dependence of the π helix is almost exclusively driven by geometric scaling effects rather than by changes in the bond strengths. Because the geometric aspects of the three helix types are roughly independent of the specific peptide sequence, the dominance of the geometric parameters may be used to rationalize why the population of π and 3_{10} helices varies with temperature[5,6] as well as to explain why the π-helical motif is the least common of the helical conformations in proteins.

References and Notes

(1) Creighton, T. E. *Proteins: Structures and Molecular Properties*, 2nd ed.; W.H. Freeman and Company: New York, 1993.
(2) Barlow, D. J.; Thornton, J. M. *J. Mol. Biol.* **1998**, *201*, 601.
(3) Weaver, T. M. *Protein Sci.* **2000**, *9*, 201.
(4) Cartailler, J.-P.; Luecke, H. *Structure* **2004**, *12*, 133.
(5) Mikhonin, A. K.; Asher, S. A. *J. Am. Chem. Soc.* **2006**, *128*, 13789.
(6) Mikhonin, A. K.; Asher, S. A.; Bykov, S. V.; Murza, A. *J. Phys. Chem.* **2007**, *B111*, 3280.
(7) Rohl, C. A.; Doig, A. J. *Protein Sci.* **1996**, *5*, 1687.
(8) Feig, M.; MacKerell, A. D.; Brooks, C. L. *J. Phys. Chem.* **2003**, *B*107, 2831.
(9) Improta, B.; Barone, V.; Kudine, K. N.; Scuseria, G. E. *J. Am. Chem. Soc.* **2001**, *123*, 3311.
(10) Wu, Y.-D.; Zhao, Y.-L. *J. Am. Chem. Soc.* **2001**, *123*, 5313.
(11) Ireta, J.; Neugebauer, J.; Scheffler, M.; Rojo, A.; Galván, M. *J. Phys. Chem.* **2003**, *B*107, 1432.
(12) Wieczorek, R.; Dannenberg, J. J. *J. Am. Chem. Soc.* **2003**, *125*, 14065.
(13) Ismer, L.; Ireta, J.; Boeck, S.; Neugebauer, J. *Phys. Rev.* **2005**, *E71*, 31911.
(14) Lee, S.; Krimm, S. *Biolpolymers* **1998**, *46*, 283.
(15) Boeck S. et al., in preparation; http://www.sfhingx.de.
(16) Perdew, J. P.; Burke, K.; Ernzerhof, M. *Phys. Rev. Lett.* **1996**, *77*, 3865.
(17) Ireta, J.; Neugebauer, J.; Scheffler, M.; Rojo, A.; Galván, M. *J. Am. Chem. Soc.* **2005**, *127*, 12741.
(18) Wieczorek, R.; Dannenberg, J. J. *J. Am. Chem. Soc.* **2005**, *127*, 14534.
(19) Savin, A. V.; Manevitch, L. I. *Phys. Rev.* **2000**, *E61*, 7065.
(20) Christiansen, P. L.; Zolotaryuk, A. V.; Savin, A. V. *Phys. Rev.* **1997**, *E56*, 877.
(21) Ismer, L.; Ireta, J.; Neugebauer, J., to be published.